Electrochimica Acta 268 (2018) 187–194

Contents lists available at ScienceDirect

Electrochimica Acta

journal homepage: www.elsevier.com/locate/electacta

About the species formed during the electrochemical half oxidation of polyaniline: Polaron-bipolaron equilibrium

Juliana Scotto, M. Inés Florit, Dionisio Posadas*

Instituto de Investigaciones Fisicoquímicas Teóricas y Aplicadas (INIFTA), Facultad de Ciencias Exactas, Universidad Nacional de La Plata, CCT La Plata-CONICET, Sucursal 4, Casilla de Correo 16, 1900 La Plata, Argentina

ARTICLE INFO

Article history:
Received 15 October 2017
Received in revised form
6 February 2018
Accepted 12 February 2018
Available online 14 February 2018

Keywords:
Polyaniline
Spectroelectrochemistry
Polarons
Capacitive currents

ABSTRACT

The UV–Vis spectra of polyaniline (Pani) films were measured in the range 200 nm–900 nm, at constant potential as well as sweeping the potential. Both free standing films and Pani films deposited on ITO substrates were employed. These measurements were carried out at different electrolyte pHs, covering the range $-0.6 < pH < 3.0$. The experimental results were analyzed considering two potential regions: that corresponding to the occurrence of the faradaic reaction; and that corresponding to the purely capacitive response. The oxidation of the leucoemeraldine form to the emeraldine form leads to the formation of two species that could be associated to bipolarons and a polaron lattice. The experimental data show that these two species are in chemical (not electrochemical) equilibrium with each other. It is shown that bipolarons convert into a polaron lattice and that this conversion is favoured by the external applied potential, in order to satisfy the charge requirements at the polymer fibril/internal solution interface. In this way, the nature of the capacitance of Pani can be explained.

1. Introduction

The electrochemical behaviour of polyaniline has attracted the attention of many workers because of its complexity and the insulator - conductor transition of this material.

Much effort has been done in understanding the oxidation mechanism of Pani films and the nature of the species involved in it; particularly, in those species related to the conductive properties of the resulting half oxidized state of Pani, and the nature of the capacitive currents present in its voltammetric response. To this end, a variety of *in situ* and *ex situ* techniques have been employed such as voltammetry, spectroelectrochemistry, EIS, EPR, conductivity, etc. [1].

Also, the electronic structure of Pani has been much investigated. This task has been carried out by quantum chemistry calculations (see, for instance [2–11]) and the results have been tested by UV–Vis spectroscopy (see, for instance [12–18]). The latter has been mostly carried out *ex situ*, in controlled atmosphere and without potential control. The quantum chemistry calculations have been performed by different computational methods in vacuum and mostly on isolated chains of limited length.

As an outcome of these experiments and calculations, it deserves to point out that two tables have been published in the literature that summarize the frequency assignments to the different forms of Pani at different protonation and oxidation states [17–19]. Also, it is important to remark that the peak frequencies as well as the theoretically predicted spectra agrees reasonably well with those obtained experimentally in vacuum in the absence of applied potential. On the other hand, the absorption spectra obtained *ex situ* in gas atmosphere are very similar to the *in situ* ones (Fig. 1).

Some time ago it was proposed that the oxidation of leucoemeraldine (LE) leads to the formation of polarons (P), at low doping levels, which can be further oxidized to bipolarons (BP) at higher doping levels (see for instance Ref. [20]), as it happens with other conductive polymers such as polypyrrole and polyacetylene. This conclusion was challenged by several workers that proposed that bipolarons are generated in a first step of the oxidation and that their instability leads to the formation of polarons by an internal conversion. Finally, they separate into a polaron lattice (PL) [4,5] that would be the species responsible for the charge transport in the polymer. All these structures are represented in Fig. 2.

Ever since, there has been many theoretical works employing more powerful methods of calculus [6–9] and including, for

* Corresponding author.
E-mail address: dposadas@inifta.unlp.edu.ar (D. Posadas).

https://doi.org/10.1016/j.electacta.2018.02.066
0013-4686/

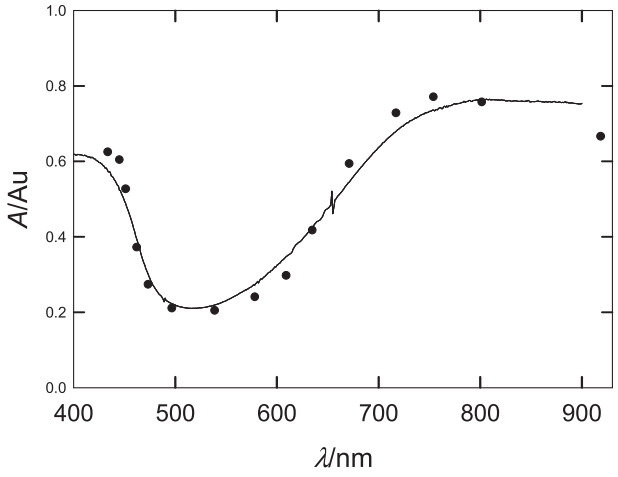

Fig. 1. Comparison of the spectra of Pani free standing films: (•) *ex situ* (data taken from Ref. [5], and (—) *in situ*. *Ex situ* films were emeraldine base treated with HCl. *In situ* films were deposited on ITO and measured at 0.45 V in 3.7 M H_2SO_4.

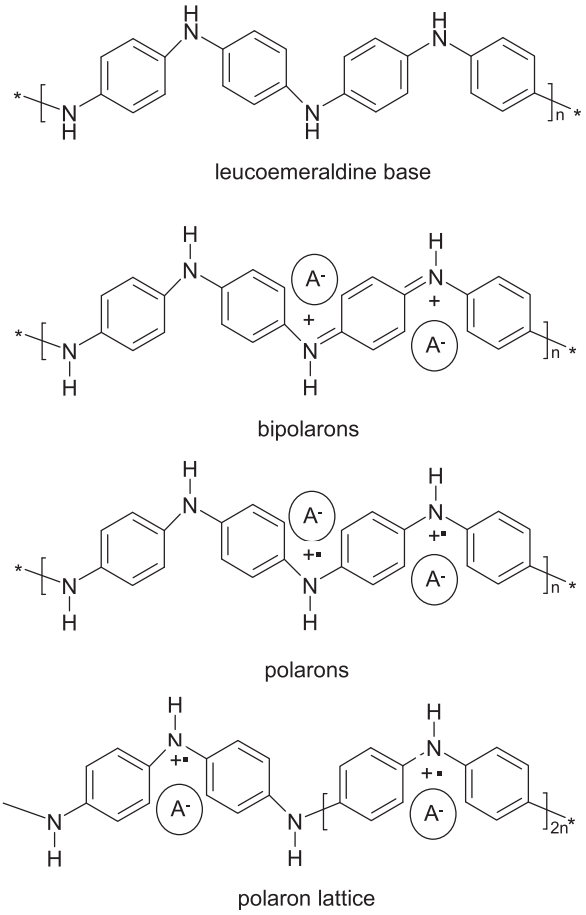

Fig. 2. Structures of leucoemeraldine base and emeraldine salt in its different forms: bipolarons, polarons and polaron lattice.

instance, protons and the corresponding counter ions [6]. A very useful account of more recent research is given in Ref. 9. However, as mentioned by Bernard and Hugot-Le Goff, besides the amine, imine and polaron sites, it is necessary to consider partially charged nitrogen atoms that do not belong exactly to these categories [21].

From the experimental viewpoint, the oxidation products absorb at about λ ≈ 400–440 nm and λ ≈ 750–800 nm, generating broad bands that are surely composed of two or more other contributions. There is general consensus about the species absorbing at 750–800 nm being the PL, whereas those absorbing at 440 nm are BPs [18].

Although most of the works show a good agreement between the calculated and the experimental data for the different species, there is still no consensus about how many chemically different species forms as products of the oxidation of leucoemeraldine, and which ones are the carriers, that is, the species actually responsible for the charge transport and the capacity of the polymer. Moreover, other workers associate the conductivity of Pani with electrons and trapped ions [22–24].

In this work, we combine spectroscopic and electrochemical measurements to show that the charge of the double layer and the conductivity of the polymer are related to the formation of chemical structures that can be followed by UV–Vis spectroscopy. Also, it is proposed that two forms of emeraldine (E) are generated from the beginning of the oxidation reaction and that they are in chemical equilibrium. These species can be associated with BP and PL, and the latter would be the responsible for the conduction in the polymer.

In the present study, we measured Pani UV–Vis spectra in the range 200 nm–900 nm; both at fixed potential and sweeping it at selected fixed wavelengths. Free standing Pani films and Pani films deposited on ITO substrates were employed. The measurements were carried out at different pHs in the range $-0.6 < pH < 3.0$.

2. Experimental

Pani films were electrosynthesized onto ITO (Indium Tin Oxide) plates ($R_s = 5–15\ \Omega$ cm, Delta Technologies). These plates were prepared as described in a previous work [25]. The active area of the polymer film onto the ITO plate was around 1.0 cm^2. The electrosynthesis was carried out by cycling the potential at 0.1 V s^{-1} between −0.2 V *vs.* SCE and a positive potential limit set at the beginning of the monomer oxidation (around 0.7 V – 0.8 V). To improve the adherence and homogeneity of the film, after a few cycles, the positive potential limit was decreased. After the synthesis, the films were washed with pure water and cycled in 3.7 M H_2SO_4 solution during some minutes and then introduced in the spectrophotometric cell. This was a square quartz cell (Spectrocell, 1 cm side) in which the electrode was inserted perpendicular to the light path. Inside the cell it was placed a Pt plate that served as the counter electrode, and a fine capillary connected to an external reference electrode. This was a saturated calomel electrode (SCE). All potentials in the text are referred to this electrode.

Free standing films were obtained by electrosynthesis of the polymer on ITO as described above. Then, they were detached from the ITO plates by applying a potential of about −1 V *vs.* SCE. Afterwards, they were placed onto a Pt gauze of 1 cm^2 area that worked as support and electrical contact. The ensemble was placed in the quartz cell as described above for the ITO plates.

Solutions were made of Milli-Q purified water, NaOH and H_2SO_4 (Carlo Erba, RPE-ACS). The latter were employed as received. A potentiostat PARC Model 273 equipped with a data logger Dataq DI-710-UH was employed for all the electrochemical experiments. The potential was varied in the range $-0.2\ V < E < 0.45$ V. Spectra were taken with an Agilent model 8453E diode array spectrophotometer. For the films deposited on ITO the spectral range was comprised between 300 nm and 900 nm, and for the free standing films between 200 nm and 900 nm.

Electrolytic solutions of different pH and constant ionic strength of 3.7 M of $H_2SO_4 + NaHSO_4$, were employed. The pH of these solutions was previously measured with a glass electrode (Ross, Orion

Research) by using a pH-meter (Cole-Palmer 59003-15). For the more acidic solutions, also a Pd (Pd) electrode was employed to check the glass electrode readings [26].

Two types of experiments were carried out. For the first ones (stationary experiments) it was applied a constant potential and spectra were taken. For the second ones (dynamic experiments) the wavelength was kept constant while sweeping the potential. Before starting the stationary experiments, with each one of the solutions of different pH values, the Pani covered electrodes were potential cycled between −0.2 V and 0.45 V for some minutes to achieve a stationary current profile. The potential was increased in steps of 0.01 V in the range between −0.2 V and 0.45 V and the spectrum was recorded at each fixed potential value. In the dynamic experiments the potential was cycled between −0.2 V and 0.45 V at different scan rates. At the same time the absorbance and current responses were measured. As a measure of the film thickness, it was employed the integrated charge from $E = -0.2$ V up to 0.45 V, Q_T (0.45) [27]. The charge was about 5 mC cm^{-2} for the films deposited on ITO and 50 mC cm^{-2} for the free standing films.

3. Results and discussion

For future reference we show in Fig. 3 the characteristic voltammetric response of Pani films deposited on ITO substrates in acid media. The current *vs.* potential responses of the free standing Pani films are coincident.

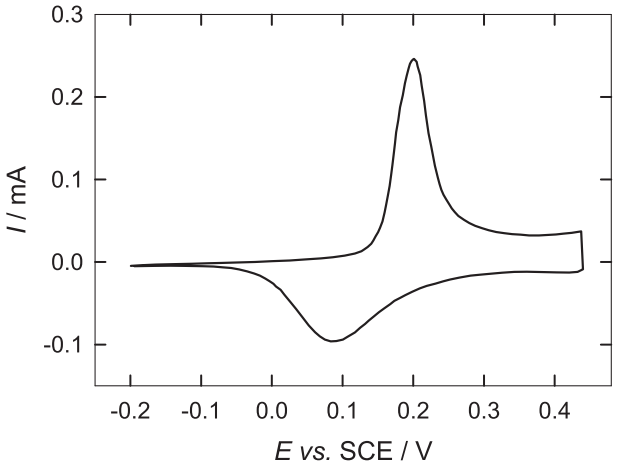

Fig. 3. Current *vs.* potential response of a Pani film deposited on ITO. $v = 5$ mVs^{-1}, 3.7 M H_2SO_4. $Q_T = 5$ mC cm^{-2}.

During the anodic scan a current peak appears at about $E \approx 0.2$ V corresponding to the oxidation of LE to E. As a consequence of the capacity of the polymer, after the faradaic process is finished, there is a current *plateau*. On inverting the potential scan direction, the capacitive current remains constant until the reduction of E to LE occurs. The peak potential corresponding to this process does not coincide with the corresponding oxidation peak.

3.1. Spectral studies at fixed potential

3.1.1. Dependence of the spectra on the applied potential

The spectra of an aniline solution (Fig. 4a) is compared with the spectra of Pani free standing membranes (Fig. 4b), at different applied potentials in 3.7 M H_2SO_4 solutions, in the range 200 nm < λ < 900 nm. It is observed that the characteristic peaks of the benzenoid bands, corresponding to the π → π* transitions, at λ ≈ 213 nm and 266 nm, are present in both figures. However, the intensity relation between them is different. In Fig. 4b, it is seen that these two bands are potential independent. The three remaining absorption bands depend on the potential: the band at about λ ≈ 320 nm decreases as the applied potential increases, therefore we will assign this band to the reduced state. The other two broad bands, at about λ ≈ 400 nm and in the region comprised between 750 nm–800 nm, increase with the applied potential. These two bands are associated to the oxidized state.

In Fig. 5, the difference spectra for a Pani film in H_2SO_4 3.7 M are shown. These are the difference between the absorbance at a particular potential value, minus the absorbance at $E = -0.2$ V.

It is convenient to observe the spectra in two potential regions: the first one is the potential region in which the faradaic process occurs (-0.2 V < E < 0.3 V); the second one corresponds to the potential region in which the capacitive current is the only contribution (0.3 V < E < 0.45 V) (see Fig. 3).

In Fig. 6a, it is shown that in the region -0.2 V < E < 0.3 V there are two bands that decrease as the potential increases: the first one centred at 320 nm and a second one centred at about 550 nm. This means that the species responsible of these absorption bands disappear as the polymer is oxidized. Both bands at 440 nm and 750 nm increase with the potential in this region.

In the region comprised between 0.3 V < E < 0.45 V it is observed that the absorbance at 400 nm decreases and the band at 750 nm increases as the potential increases (Fig. 6b). Actually, it is appreciated that the band at 400 nm is composed of at least two

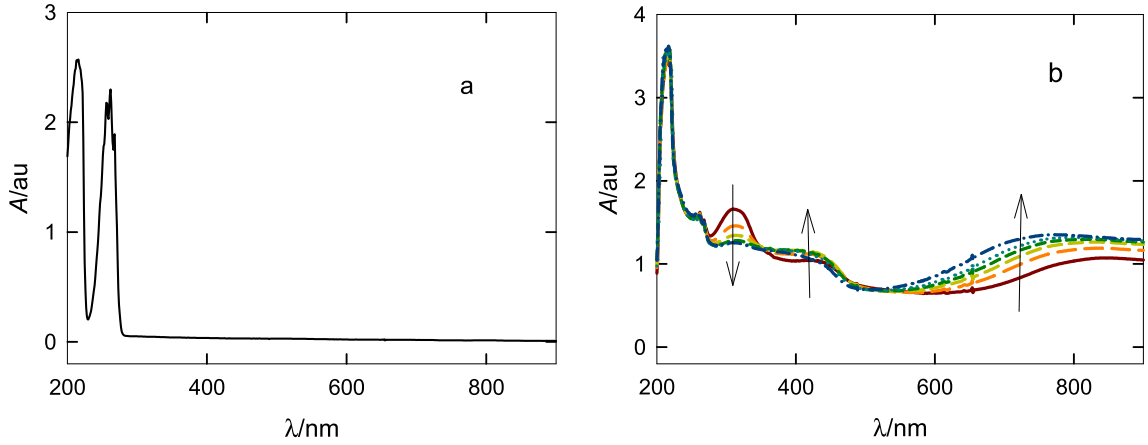

Fig. 4. UV- Visible spectra of: (a) Aniline solution in H_2SO_4; (b) Free standing membrane of Pani in H_2SO_4 solutions at different applied potentials. (——) 0.1 V, (— — —) 0.2 V, (— — —) 0.25 V, (- - -) 0.3 V, (· · · · · ·) 0.35 V, (— · — · —) 0.45 V. $Q_T = 50$ mCcm^{-2}. The arrows indicate the direction of increasing potentials.

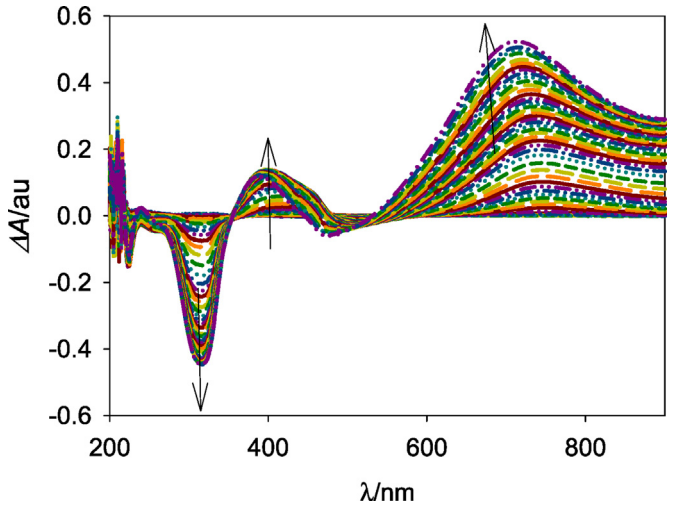

Fig. 5. Difference spectra of a Pani free standing film in 3.7 M H_2SO_4 solution at different applied potentials in the range between−0.2 V and 0.45 V. $Q_T = 50$ mCcm^{-2}. The arrows indicate the direction of increasing potentials.

bands: one peaking at about 390 nm and another around 440 nm.

An enlargement of the difference spectra is shown in Fig. 7a and b for wavelengths between 340 nm and 500 nm. There, it is clearly seen that, beyond $E = 0.3$ V, the second component of the band at 400 nm decreases as the potential increases.

These results show that, even in a potential range where the current is purely capacitive, the absorbance changes with the potential, meaning that the charge of the double layer of the polymer must be related to chemical species with absorption bands at 400 nm and 750 nm.

3.1.2. Dependence of the crossing points on the applied potential

The presence of three isosbestic points, at about $\lambda_{c1} \approx 395$ nm, $\lambda_{c2} \approx 500$ nm and $\lambda_{c3} \approx 600$ nm can be observed in Fig. 6a. These points are generated by the potential change and they refer to an electrochemical equilibrium between the reduced and oxidized Pani.

In Fig. 6b, a crossing point at about 550 nm is also seen. It occurs as a consequence of the decrease of the second component of the band at 400 nm and an increase of the band at 750 nm, as the potential increases. Since this crossing point happens outside the potential range where the faradaic reaction occurs, it should not involve an electrochemical (Nerstian) equilibrium but rather other type of potential dependence. Clearly, this equilibrium involves at least two species of oxidized Pani. We will call the species responsible of the decrease of the absorbance at 400 nm, Ox_1; and that responsible of the increase of the absorbance at 750 nm, Ox_2. According to the frequency assignments to the different structures of Pani given in the bibliography [18] Ox_1 and Ox_2 can be associated to BPs and PL, respectively. However, the conclusions obtained below are independent of this band assignation, so we will retain this notation.

3.2. Voltabsorptiometric studies at fixed wavelength

Absorbance measurements were made at fixed wavelength, at different sweep rates. Three wavelengths were chosen corresponding to the main absorption regions in the spectra: $\lambda = 320$ nm, $\lambda = 400$ nm and $\lambda = 750$ nm. At all λs, the voltabsorptiograms do not depend on the sweep rate in the range $0.001\ V^{-1} < \nu < 0.05\ V^{-1}$. Moreover, if during the potential sweeping, the potential is held at different values, for several minutes, the absorbance remains constant. The trace is recovered as the potential is released.

The absorbance as a function of E is shown in Fig. 8. It is observed that the traces of the anodic sweep, at the three wavelengths, are similar in shape in the potential range comprised between −0.2 V and 0.25 V. This is precisely the potential range in which the faradaic process occurs. In the potential region corresponding to the purely capacitive response the absorbance at 320 nm remains almost constant. For the other two wavelengths, as noted by previous workers [12,15], the absorbance either *linearly* decreases (at 400 nm) or increases (at 750 nm) with the potential. The slopes, dA/dE, measured at $\lambda = 400$ nm and 750 nm, are but slightly dependent on the pH.

The derivative of A with respect to E allows obtaining the voltabsorptiograms. In Fig. 9 are shown the normalized voltabsorptiograms at 320 nm, 400 nm and 750 nm in 3.7 M H_2SO_4.

The same plots were made at all pHs studied. It is interesting to note that, for the anodic sweep, the peak potentials are similar at the three wavelengths for the more acidic solutions. Some differences are noted as the pH increases. During the cathodic sweep the peak potentials are different at all pHs and again the differences are more evident for the higher pHs. On the other hand, it is observed that, in the potential region corresponding to the capacitive current, dA/dE values drop almost to zero at 320 nm, whereas it becomes negative at 400 nm and positive at 750 nm. Reversing the direction of the potential scan, dA/dE changes sign, so that it becomes positive at 400 nm and negative at 750 nm. All these results are a further proof that there is more than one process occurring

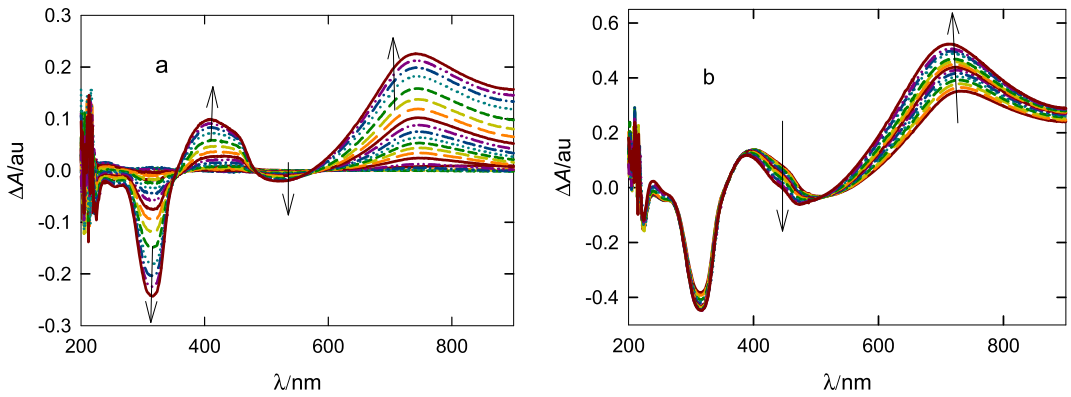

Fig. 6. Difference spectra in different potential ranges: (a) − 0.2 V < E < 0.3 V and (b) 0.3 V < E < 0.45 V. The experimental conditions are the same as in Fig. 5.

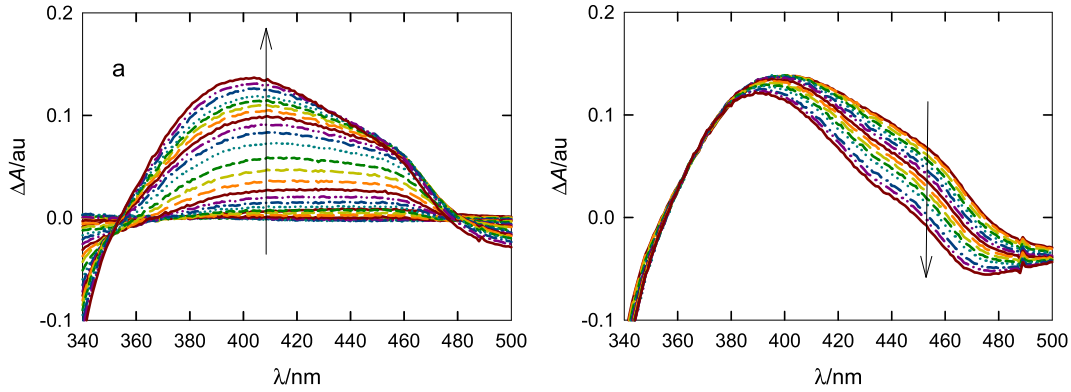

Fig. 7. Enlargement of the difference spectra shown in Fig. 6 for the spectral region between 340 nm and 500 nm. (a) Applied potentials in the range – 0.2 V < E < 0.3 V and (b) Applied potentials in the range 0.3 V < E < 0.45 V.

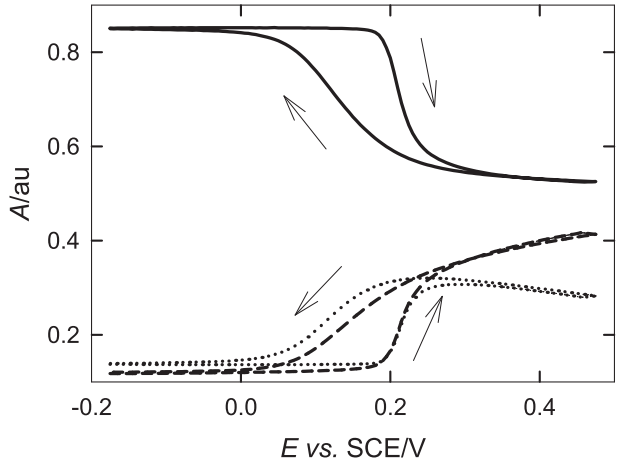

Fig. 8. Absorbance as a function of potential for a Pani film deposited on ITO in 3.7 M H_2SO_4 solution, at different wavelengths: (—) 320 nm, (…..) 400 nm and (- - -) 750 nm $v = 0.005\ V^{-1}$. The arrows indicate the potential scan direction. $Q_T = 5\ mC\ cm^{-2}$.

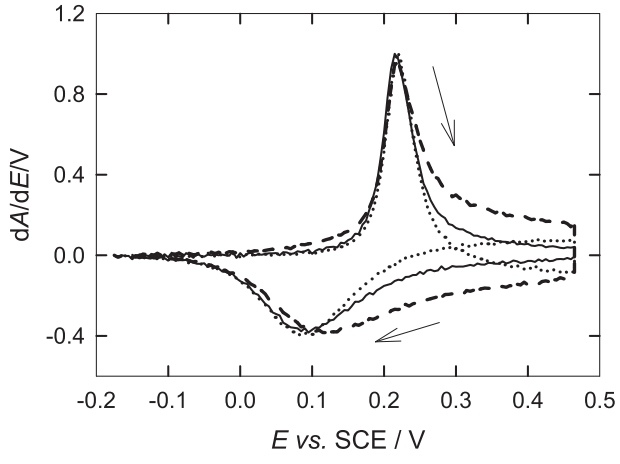

Fig. 9. Normalized voltabsorptiograms at (—) 320 nm, (…..) 400 nm and (- - -) 750 nm. The arrows indicate the direction of the potential sweep. The experimental conditions are the same as in Fig. 8.

simultaneously and that the species generated during of the oxidation of Pani are involved in at least two equilibriums that have different dependences with the potential.

3.3. Relation between the absorbance at different wavelengths

The presence of an isosbestic point in Fig. 6a (−0.2 V < *E* < 0.3 V) shows an electrochemical equilibrium between the reduced and the oxidized Pani. On the other hand, the isosbestic point in Fig. 6b (0.3 V < *E* < 0.45 V) suggests there are two oxidized species in equilibrium (Ox_1 and Ox_2). Therefore we may write the reaction scheme as:

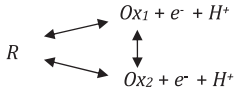

The absorbance at any wavelength, A^λ, is the sum of the absorbance of the three species.

$$A^\lambda = A^\lambda_R + A^\lambda_{Ox1} + A^\lambda_{Ox2} \quad (1)$$

Employing Beer's law, $A^\lambda_i = \varepsilon^\lambda_i l c_i$,

$$A^\lambda = \varepsilon^\lambda_R l c_R + \varepsilon^\lambda_{Ox1} l c_{Ox1} + \varepsilon^\lambda_{Ox2} l c_{Ox2} \quad (2)$$

where l is the optical path and ε^λ_i, the molar absorption coefficient of species *i*. Assuming that the total concentration of redox sites (reduced and oxidized), c_T, is constant or, in terms of the concentration fractions, $x_i = c_i/c_T$:

$$c_T = c_R + c_{Ox1} + c_{Ox2} \quad (3)$$

$$1 = x_R + x_{Ox1} + x_{Ox2} \quad (4)$$

Eq. (2) may be written in terms of x_i, as:

$$\frac{A^\lambda}{l c_T} = \varepsilon^\lambda_R x_R + \varepsilon^\lambda_{Ox1} x_{Ox1} + \varepsilon^\lambda_{Ox2} x_{Ox2} \quad (5)$$

Writing Eq. (5) for the three wavelengths employed here and eliminating the concentration fractions between the three resulting equations, it is obtained:

$$a\left(\frac{A^{400}}{l c_T} - \varepsilon^{400}_R\right) + b\left(\frac{A^{750}}{l c_T} - \varepsilon^{750}_R\right) - \left(\frac{A^{320}}{l c_T} - \varepsilon^{320}_R\right) = 0 \quad (6)$$

where

$$a = \frac{(\varepsilon^{320}_{ox2} - \varepsilon^{320}_R)(\varepsilon^{750}_{ox1} - \varepsilon^{750}_R) - (\varepsilon^{320}_{ox1} - \varepsilon^{320}_R)(\varepsilon^{750}_{ox2} - \varepsilon^{750}_R)}{(\varepsilon^{750}_{ox1} - \varepsilon^{750}_R)(\varepsilon^{400}_{ox2} - \varepsilon^{400}_R) - (\varepsilon^{750}_{ox2} - \varepsilon^{750}_R)(\varepsilon^{400}_{ox1} - \varepsilon^{400}_R)}$$

and:

$$b = \frac{(\varepsilon_{ox1}^{320} - \varepsilon_R^{320})(\varepsilon_{ox2}^{400} - \varepsilon_R^{400}) - (\varepsilon_{ox2}^{320} - \varepsilon_R^{320})(\varepsilon_{ox1}^{400} - \varepsilon_R^{400})}{(\varepsilon_{ox1}^{750} - \varepsilon_R^{750})(\varepsilon_{ox2}^{400} - \varepsilon_R^{400}) - (\varepsilon_{ox2}^{750} - \varepsilon_R^{750})(\varepsilon_{ox1}^{400} - \varepsilon_R^{400})}$$

Deriving Eq. (6) with respect to E, allows obtaining:

$$\frac{\partial A^{320}}{\partial E} = a\frac{\partial A^{750}}{\partial E} + b\frac{\partial A^{400}}{\partial E} \quad (7)$$

Data of Fig. 9 for A at 400 nm and 750 nm may be fitted to the data at 320 nm to obtain the coefficients a and b. The values of coefficients obtained are but slightly dependent on the pH; this may be due to small changes in the molar absorption coefficients values with the increase of the pH.

In Fig. 10 are compared the dA/dE values calculated with parameters resulting from the fit, and the experimental ones, at two pH values.

This procedure shows that the absorbance of the species disappearing at 320 nm is proportional to those appearing at 400 nm and 750 nm. Therefore, the reaction scheme proposed above correctly represents the experimental results. Also, it should be remarked that Eq. (7) is fulfilled at all the potentials and for both scan directions. Taking into account the assignation of the bands, this means that, during the faradaic reaction, both BPs and PL are generated as products of leucoemeraldine oxidation and there is a chemical equilibrium between these species that depends on the potential.

3.4. Nature of the capacitance

It is well known that, in acid solutions, as the polymer oxidizes its conductivity steadily increases [28–31], and has a maximum at about 0.45 V (SCE). Since the concentration of Ox_2 (PL) increases with the potential, it is proposed that this one is the species responsible for the conduction.

Barsukov and Chivikov [32] suggested that the formation of a PL is related to the charging of the double layer. Assuming that this is the carrier species we will try to prove this assertion.

Let us first consider the capacitance in the potential region between $0.3\,V < E < 0.45\,V$. Within this range, the double layer charging is the only process that takes place; that is, there is no charge transfer. Moreover, this capacitance depends linearly with the amount of polymer; therefore, it is a bulk process [33]. Also, it has been suggested, in order to explain the unusually high values of the interfacial capacity, that the locus of this double layer must be at the polymer fibril/solution interface within the bulk of the polymer.

In this work, it has been shown that in this potential region there are two species whose concentration depends on the applied potential, thus, they should be associated with the double layer charging. If the double layer charging were associated to free electrons, *i.e.* the conduction mechanism was like in a metal, they would not be seen in the absorbance measurements. Here we propose that, as the potential is increased in this range, the amount of carriers required to charge the double layer increases. This increment is provided by a displacement of the equilibrium BP ↔ PL in favor of the latter. Incidentally, this would also explain why the absorbance at 750 nm (mainly associated to the PL) increases linearly with the potential whereas the absorbance at 400 nm (mainly associated with the BP) decreases linearly with the potential. Moreover, as commented above (Section 3.2), the changes of the slopes dA/dE, measured at $\lambda = 400$ nm and 750 nm, are but slightly dependent on the pH. This is in agreement with the fact that, as we shown in a previous work, the double layer capacity is independent of the pH in the range $-0.6 < pH < 2.0$ [34].

From the above arguments, it is clear why the isosbestic point mentioned in relation to Fig. 6b is related not to a Nersntian equilibrium, but rather to a chemical equilibrium driven by the potential.

3.5. Relation between the voltammetric charge and the absorbance

In this section it will be shown that the absorbance at any wavelength can be expressed in terms of the potential and the faradaic oxidation fraction. About twenty years ago, in order to explain the shape of the voltammetric response of conducting polymers, Feldberg proposed a model in which the total charge, Q_T, is the sum of a faradaic, Q_F, and a capacitive, Q_C, contributions [35]. From this model it is possible to calculate the faradaic oxidation degree, x_{Ox}, from voltammetric measurements [34]:

$$Q_T(E) = x_{Ox}(E)C_d(\sigma + E) \quad (8)$$

Where C_d and $C_d\,\sigma$ are the slope and ordinate respectively of the linear portion of the $Q_T(E)$ *vs.* E plot [34].

In this work it is proposed that the capacitive charge is proportional to the concentration of Ox_2 (PL) sites. That is:

$$Q_C = g x_{ox2} \quad (9)$$

where g is a proportionality constant. Assuming, as before, that there are only three species: R, Ox_1 and Ox_2 and that $1 = x_R + x_{Ox1} + x_{Ox2}$ (Eq. (4)), it is possible to show that (see Appendix):

$$\frac{A^\lambda}{lc_T} - \varepsilon_R^\lambda = x_{Ox}C_d'\left(\sigma' + E\right) \quad (10)$$

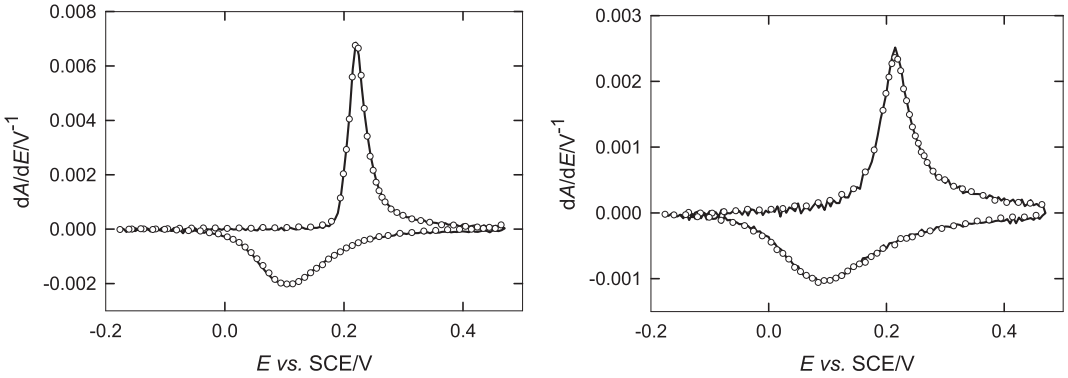

Fig. 10. Comparison of the voltabsorptiograms at $\lambda = 320$ nm (—) with those calculated from the fit (○), at two different pHs: (a) – 0.60, (b) 0.56. $Q_T = 5\,mC\,cm^{-2}$.

where $C_d' = C_d\frac{(\varepsilon_{ox2}^{\lambda}-\varepsilon_{ox1}^{\lambda})}{g}$ and $\sigma' = \frac{g(\varepsilon_{ox1}^{\lambda}-\varepsilon_R^{\lambda})}{C_d(\varepsilon_{ox2}^{\lambda}-\varepsilon_{ox1}^{\lambda})} - E_z$. Ez is the zero charge potential of the polymer [35]. Eq. (10) shows that, under the assumptions made above, the absorbance at any wavelength is proportional to the oxidation degree, $x_{Ox} = 1 - x_R = x_{Ox1} + x_{Ox2}$. Note the similarity between Eq. (8) and Eq. (10).

Considering the potential as the independent variable, Eq. (10) is the equation of a straight line. $lc_T C_d'$ and $lc_T(C_d'\sigma' + \varepsilon_R^{\lambda})$ are the slope and the ordinate at the origin of an *A vs. E* plot, and they can be obtained employing the experimental data of Fig. 8 by fitting a straight line to the linear portion of the plot. Then, Eq. (10) may be employed to obtain x_{Ox} from absorptiometric measurements.

Fig. 11 shows that the oxidation degree obtained at 320 nm is coincident with the voltammetric one, justifying the assumptions made in the deduction of Eq. (10). The two other wavelengths (400 and 750 nm) give identical results.

4. Conclusions

The UV- Vis spectra, both at fixed and sweeping the potential in the range 200–900 nm were measured. Both free standing Pani films as well as films deposited on ITO substrates were employed. These measurements were carried out at different pHs in the range - 0.6 < pH < 3.0.

The experimental results were analyzed considering two potential regions: (i) that corresponding to occurrence of the faradaic reaction and (ii) that corresponding to the purely capacitive response.

The analysis of the results shows that the oxidation of the leucoemeraldine form leads to the formation of two other species simultaneously that we associated to BP and PL.

The experimental data show that these two species are in chemical (not electrochemical) equilibrium with each other. Also, it is shown that beyond about 0.3 V, the absorbance of BPs and PL linearly change with the applied potential. Further, the equilibrium between them is displaced in favour of the latter by an increase of the applied external potential to satisfy the charge requirements at the fibril/internal solution interface. In this way, the nature of the capacitance of Pani can be explained.

On the other hand, we demonstrated that the capacitive charge in the polymer is proportional to the fraction of PL, and it is concluded that this is the species responsible for charge transport in the polymer.

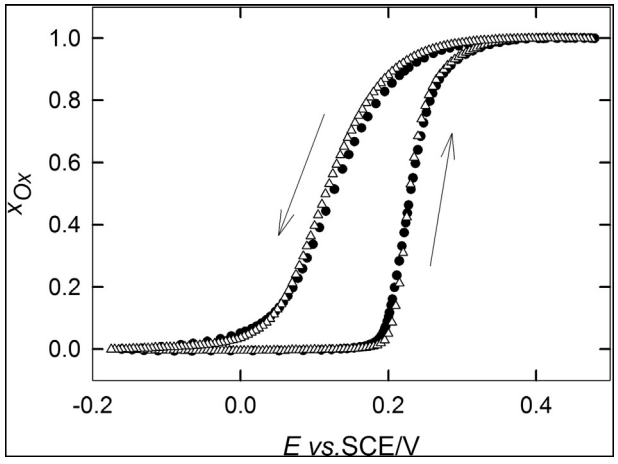

Fig. 11. Comparison of the oxidation degrees obtained from voltammetric data employing Eq. (8) (•) and those obtained from spectrometric data of Fig. 8 employing Eq. (10), at 320 nm (Δ).

Also, it is proposed an equation to describe the dependence of the absorbance at any wavelength with the oxidized fraction of the polymer. This allows obtaining the oxidation degree of the polymer from absorbance measurements.

Acknowledgments

This work was financially supported by the Consejo Nacional de Investigaciones Científicas y Técnicas (PIP 0813), the Agencia Nacional de Promoción Científica y Tecnológica (PICT-0407) and the Universidad Nacional de La Plata (Proyecto 11/X590). MIF and DP are members of the CIC of the CONICET. JS thanks a fellowship from the Agencia Nacional de Promoción Científica Tecnológica and a fellowship from the CONICET.

Appendix. Relation between the absorbance and the oxidation degree, x_{Ox}

This deduction is based on Eq. (8) in the text, in which it is assumed that the capacitive charge is proportional to the oxidation degree, x_{Ox}. Besides, it is also assumed that there are only three species present in the system, one reduced, R, and two oxidized, Ox_1 and Ox_2, that the sum of their concentrations, c_T, remains constant during the electrochemical process, and that the capacitive charge is proportional to the concentration of Ox_2 (PL) sites. In equations:

$$Q_C = g x_{ox2} \tag{A.1}$$

and

$$c_T = c_R + c_{Ox1} + c_{Ox2} \tag{A.2}$$

Then, from Eq. (5) in the text:

$$\frac{A^{\lambda}}{lc_T} = \varepsilon_R^{\lambda} x_R + \varepsilon_{Ox1}^{\lambda} x_{Ox1} + \varepsilon_{Ox2}^{\lambda} x_{Ox2} \tag{A.3}$$

Replacing $x_R = 1 - x_{Ox}$, and $x_{Ox1} = x_{Ox} - x_{Ox2}$ and grouping, we obtain:

$$\frac{A^{\lambda}}{lc_T} = \varepsilon_R^{\lambda}(1 - x_{Ox}) + \varepsilon_{Ox1}^{\lambda} x_{Ox} + \left(\varepsilon_{Ox2}^{\lambda} - \varepsilon_{Ox1}^{\lambda}\right) x_{Ox2} \tag{A.4}$$

Applying Eq. (A.1) and recalling that $x_{Ox2} = Q_C(E)g^{-1} = C_d(E - E_z)x_{Ox}(E)g^{-1}$ [34]:

$$\frac{A^{\lambda}}{lc_T} - \varepsilon_R^{\lambda} = \left[\left(\varepsilon_{ox1}^{\lambda} - \varepsilon_R^{\lambda}\right) + \left(\varepsilon_{ox2}^{\lambda} - \varepsilon_{ox1}^{\lambda}\right) g^{-1} C_d (E - E_z)\right] x_{ox} \tag{A.5}$$

References

[1] P. Chandrasekhar, Conducting Polymers: Fundamentals and Applications, Kluwer Academic Publishers, Boston, 1999.
[2] B. Sjögren, S. Stafström, Electronic excitations in polyaniline: an INDO/S-CI study, J. Chem. Phys. 88 (1988) 3840–3847.
[3] Z.T. de Oliveira, M.C. dos Santos, Semi-empirical study of chain conformation and absorption spectra of polyanilines: size, solvent and disorder effects, Chem. Phys. 260 (2000) 95–103.
[4] A.G. Epstein, A.J. Ginder, J.M. Ritcher, A.F. MacDiarmid, in: L. Alcácer (Ed.), Conducting Polymers, D. Reidel Publishing Company, Dordrecht, 1987.
[5] S. Stafström, J.L. Brédas, A.J. Epstein, H.S. Woo, D.B. Tanner, W.S. Huang, A.G. MacDiarmid, Polaron lattice in highly conducting polyaniline, Phys. Rev. Lett. 59 (1987) 1464.
[6] C. Cavazzoni, R. Colle, R. Farchioni, G. Grosso, HCl-doped conducting Emeraldine polymer studied by ab initioCar-Parrinello molecular dynamics, Phys. Rev. B 74 (2006) 33103.
[7] A. Varela Álvarez, J.A. Sordo, G.E. Scuseria, Doping of polyaniline by acid-base chemistry: density functional calculations with periodic boundary conditions,

J. Am. Chem. Soc. 127 (2005) 11318–11327.
[8] C. Alemán, C.A. Ferreira, J. Torras, A. Meneguzzi, M. Canales, M.A.S. Rodrigues, J. Casanovas, On the molecular properties of polyaniline: a comprehensive theoretical study, Polymer 49 (2008) 5169–5176.
[9] M. Canales, J. Torras, G. Fabregat, A. Meneguzzi, C. Alemán, Polyaniline emeraldine salt in the amorphous solid state: polaron versus bipolaron, J. Phys. Chem. B 118 (2014) 11552–11562.
[10] R. Colle, P. Parruccini, A. Benassi, C. Cavazzoni, Optical properties of emeraldine salt polymers from ab initio calculations : comparison with recent experimental data, Phys. Rev. B 111 (2007) 2800–2805.
[11] C. Cavazzoni, R. Colle, R. Farchioni, G. Grosso, Acidification of three-dimensional emeraldine polymers: search for minimum energy paths from base to salt, J. Chem. Phys. 128 (2008), 234903.
[12] T. Kobayashi, H. Yoneyama, H. Tamura, Electrochemical reactions concerned with electrochromism of polyaniline film-coated electrodes, J. Electroanal. Chem. 177 (1984) 281–291.
[13] R.J. Cushman, P.M. McManus, S. Cheng Yang, Spectroelectrochemical study of polyaniline: the construction of a pH-potential phase diagram, J. Electroanal. Chem. 219 (1987) 335–346.
[14] E.M. Genies, M. Lapkowski, Spectroelectrochemical study of polyaniline versus potential in the equilibrium state, J. Electroanal. Chem. 220 (1987) 67–82.
[15] D. Stilwell, S.M. Park, Electrochemistry of conductive polymers V. In situ spectroelectrochemical studies of polyaniline films, J. Electrochem. Soc. 136 (1989) 427–433.
[16] A. Neudeck, A. Petr, L. Dunsch, The redox mechanism of polyaniline studied by simultaneous ESR-UV-vis spectroelectrochemistry, Synth. Met. 107 (1999) 143–158.
[17] D. Chinn, J. DuBow, J. Li, J. Janata, M. Josowicz, Comparison of chemically and electrochemically prepared polyaniline films. 2. Optical properties, Chem. Mater. 7 (1995) 1510–1518.
[18] A.A. Nekrasov, V.F. Ivanov, A.V. Vannikov, Analysis of the structure of polyaniline absorption spectra based on spectroelectrochemical data, J. Electroanal. Chem. 482 (2000) 11–17.
[19] A. a. Nekrasov, V.F. Ivanov, A.V. Vannikov, Effect of pH on the structure of absorption spectra of highly protonated polyaniline analyzed by the Alentsev-Fock method, Electrochim. Acta 46 (2001) 4051–4056.
[20] E.M. Genies, M. Lapkowski, Spectroelectrochemical study of polyaniline versus potential in the equilibrium state, J. Electroanal. Chem. 220 (1987) 67–82.
[21] M.C. Bernard, A. Hugot-Le Goff, Quantitative characterization of polyaniline films using Raman spectroscopy. I: polaron lattice and bipolaron, Electrochim. Acta 52 (2006) 595–603.
[22] J. Toušek, J. Touškova, R. Chomutová, I. Křivka, M. Hajná, J. Stejskal, Mobility of holes and polarons in polyaniline films assessed by frequency-dependent impedance and charge extraction by linearly increasing voltage, Synth. Met. 234 (2017) 161–165.
[23] V.J. Babu, S. Vempati, S. Ramakrishna, Conducting polyaniline-electrical charge transportation, Mater. Sci. Appl. 4 (2013) 1–10.
[24] J. Stejskal, O.E. Bogomolova, N.V. Blinova, M. Trchová, I. Šeděnková, J. Prokeš, I. Sapurina, Mixed electron and proton conductivity of polyaniline films in aqueous solutions of acids: beyond the 1000 S cm-1 limit, Polym. Int. 58 (2009) 872–879.
[25] W.A. Marmisollé, M.I. Florit, D. Posadas, Coupling between proton binding and redox potential in electrochemically active macromolecules. The example of Polyaniline, J. Electroanal. Chem. 707 (2013) 43–51.
[26] G.J. Hills, D.J.G. Ives, in: D.J.G. Ives, G.J. Janz (Eds.), Reference Electrodes, Academic Press, London, 1961.
[27] W.A. Marmisollé, M.I. Florit, D. Posadas, A formal representation of the anodic voltammetric response of polyaniline, J. Electroanal. Chem. 655 (2011) 17–22.
[28] E.W. Paul, A.J. Ricco, M.S. Wrighton, Resistance of polyaniline films as a function of electrochemical potential and the fabrication of polyaniline-based microelectronic devices, J. Phys. Chem. 89 (1985) 1441–1447.
[29] W.W. Focke, G.E. Wnek, Y. Wei, Influence of oxidation state, pH, and counterion on the conductivity of polyaniline, J. Phys. Chem. 91 (1987) 5813–5818.
[30] D. Ofer, R.M. Crooks, M.S. Wrighton, Potential dependence of the conductivity of highly oxidized poly thiophenes, polypyrroles, and polyaniline: finite windows of high conductivity, J. Am. Chem. Soc. 112 (1990) 7869–7879.
[31] P.M. McManus, R.J. Cushman, S. ChengYang, Influence of oxidation and protonation on the electrical conductivity of polyaniline, J. Phys. Chem. 91 (1987) 744–747.
[32] V. Barsukov, S. Chivikov, The “capacitor” concept of the current-producing process mechanism in polyaniline type conducting polymers, Electrochim. Acta 41 (1996) 1773–1779.
[33] W.A. Marmisollé, Estudsio de la Propiedades Fisicoquímicas de Macromoléculas Sintéticas Electroactivas, PhD. Thesis, Polianilina y Derivados, Facultad de Ciencias Exactas, UNLP, 2011.
[34] J. Scotto, M.I. Florit, D. Posadas, pH dependence of the voltammetric response of Polyaniline, J. Electroanal. Chem. 785 (2017) 14–19.
[35] S.W. Feldberg, Reinterpretation of polypyrrole electrochemistry. Consideration of capacitive currents in redox switching of conducting polymers, J. Am. Chem. Soc. 106 (1984) 4671–4674.